

# Performances of the LDPC-Coded Adaptive Modulation Schemes in Multi-Carrier Transmissions

Vasile Bota, Zsolt Polgar, Mihaly Varga Technical University of Cluj-Napoca, Communications Department G.Baritiu 26, 400027 CLUJ-NAPOCA, ROMANIA Vasile.Bota@com.utcluj.ro

**Abstract**— The paper presents the BER vs. SNR and throughput vs. SNR simulation performances of some transmission configurations based on LDPC-coded adaptive QAM modulations over a multi-carrier AWGN channel. The proposed configurations provide significant coding gains and increased throughput.

It also includes a brief description of the array-based LDPC codes employed and a fast LDPC-encoding algorithm. Some considerations regarding the influences of the code parameters and of the bit-loading upon the scheme's performances are discussed as well.

**Key words:** array-based LDPC codes, QAM multi-carrier transmissions; BER and throughput vs. SNR performances.

## I. PARAMETERS AND ENCODING-DECODING OF LDPC CODES

### A. Types of LDPC Codes Employed

THE LDPC codes are block codes, basically defined by three parameters  $p$ ,  $j$ , and  $k$  (integer numbers) that observe the following conditions [1]:

$$p \text{ is a prime integer, } j < k \leq p; \quad (1)$$

The codeword length  $N$ , the number of control bits  $C$ , the number of information bits  $J$  and the code ratio  $R$  are defined, respectively, by:

$$N = k \cdot p; \quad C = j \cdot p; \quad J = (k-j) \cdot p; \quad R = (k-j)/k; \quad (2)$$

The control matrix,  $H$ , of a LDPC code is a 4-cycle free sparse matrix that might take three forms, which define the three types of LDPC codes: randomly generated by computer search [2], [3], by complete array-code control matrices [3] and by triangular-shaped array-code control matrices [4].

For reasons to be explained below, this paper considers only the codes generated by a triangular-shaped array-code control matrix  $H$  ( $jp \times kp$ ).

The generic form of the triangular-shaped matrix  $H_T$  is generated, see (3), by using an elementary matrix  $a$ ,  $pxp$ , and the

unity and null  $pxp$  matrices,  $I$  and  $0$ :

$$H_T = \begin{bmatrix} I & I & I & \cdot & I & I & \cdot & I \\ 0 & I & a & \cdot & a^{j-2} & a^{j-1} & \cdot & a^{k-2} \\ 0 & 0 & I & \cdot & a^{2(j-3)} & a^{2(j-2)} & \cdot & a^{2(k-3)} \\ & & \vdots & \vdots & \vdots & \vdots & \vdots & \vdots \\ 0 & 0 & 0 & \cdot & I & a^{j-1} & \cdot & a^{(j-1)(k-1)} \end{bmatrix} \quad (3)$$

There are two types of elementary matrices  $a$  that may be employed; they can be obtained starting from the unity  $pxp$  matrix, either by shifting its rows downwards or upwards with one position.

### B. Generation of the Control Matrix $H_T$

The regular structure of the triangular-shaped matrix allows a systematic generation, starting from the code parameters  $j$ ,  $k$ ,  $p$ . Using the property of the matrix  $a$ ,  $a^p = I$  ( $pxp$ ), and the rule that gives the power of  $a$  inside the  $H_T$  (3), an algorithm to compute the indexes (row, column) defining the positions that take the logical value "1", in terms of the parameters  $j$ ,  $k$  and  $p$ , can be determined. So, the binary matrix  $H_T$  is generated by filling with "1" only on the positions given by that algorithm.

### C. Shortening the LDPC Codes

In order to adapt the number of information bits of the codeword to the information source or to adapt the codeword length, to the transmitted symbol, the LDPC codes can be shortened [1].

Supposing that  $J' < J$  is the new number of information bits, one way of obtaining the  $H_s$  matrix of the shortened code is by deleting the rightmost  $J-J'$  columns from the parent-code control matrix  $H$ .

The shortened code rate  $R'$  is smaller than the rate of the parent code  $R$ :

$$R' = J'/(J'+C) < R = J/(J+C) \quad (4)$$

### D. Encoding the LDPC Codes

Considering the codeword  $v = [c_0, \dots, c_{jp-1}, i_0, \dots, i_{(k-j)p-1}]$ , the control bits  $c_m$  are computed in terms of the information bits  $i_i$

by solving the C equations system:

$$H \cdot v^t = 0 \quad (5)$$

This approach has two major shortcomings:

- for great values of parameters  $j$  and/or  $p$ ,  $C$  becomes large implying a significant computational load that increases the processing time and/or the hardware required by the implementation;

- it requires all information bits  $i_l$ ,  $l = 0, \dots, (k-j)p-1$  at the same time; this requirement induces a one-codeword additional latency in the system.

These shortcomings may be avoided by a simpler and faster encoding method, briefly described below.

The  $(jp \times kp)$  HT matrix is split into two matrices  $D$  and  $E$ , by retaining the first  $jp$  columns into matrix  $D$  and the rest of the  $(kp-jp)$  columns into matrix  $E$ . Consequently, the two matrices have the following dimensions:  $D - (jp \times jp)$ ;  $E - ((kp-jp) \times jp)$  (7). The  $D$  matrix is square and has a non-zero determinative, see (3). So, the encoding equation (5) may be transformed as:

$$\begin{aligned} [H] \cdot [v]^t = [0] &\Leftrightarrow [D] \cdot \begin{bmatrix} c_0 \\ \vdots \\ c_{jp-1} \end{bmatrix} + [E] \cdot \begin{bmatrix} i_0 \\ \vdots \\ i_{(k-j)p-1} \end{bmatrix} = [0] \Leftrightarrow \\ &\Leftrightarrow \begin{bmatrix} c_0 \\ \vdots \\ c_{jp-1} \end{bmatrix} = [F] \cdot \begin{bmatrix} i_0 \\ \vdots \\ i_{(k-j)p-1} \end{bmatrix} \end{aligned} \quad (6)$$

By expanding the encoding matrix  $F$  ( $jp \times (k-j)p$ ) and denoting by  $[f_l]$  the columns of  $F$ , each of them a  $jp$ -bit vector, we may write (7) as:

$$[f_0] \cdot i_0 + \dots + [f_{(k-j)p-1}] \cdot i_{(k-j)p-1} = [C]; \quad (7)$$

The off-line computed encoding matrix  $F$  is stored column-by-column in the implementing device. Each information bit multiplies the column with the same index, and then the results are accumulated, giving the control bits vector  $[C]$ .

The encoding matrix of the shortened code  $F_s$  may be obtained by deleting the rightmost  $k-k'$  columns of matrix  $F$ .

This encoding algorithm is faster than the one that implies solving the system (5) and computes the control bits,  $[C]$ , in a parallel way by using one information bit for every step; this approach allows a serial employment of the information bits and, consequently, does not insert any additional latency in the system.

Equations (5) and (6) show the significance of the code parameters,  $k$  and  $j$ . Parameter  $j$  equals the number of control equations a codeword bit is involved in, while  $k$  shows the number of bits involved in a control equation.

### E. Decoding the LDPC Codes

The decoding of the LDPC codes is accomplished by using the message-passing algorithm (MP), as described in [2], which will not be described here. This algorithm, based on the Bayes criterion requires the previous computation of the a posteriori probabilities,  $F_n^0(r/0)$  and  $F_n^1(r/1)$ , for every bit of a codeword, where  $r$  denotes the received vector,  $n$  is the bit index and  $0/1$  denote the bit logical value.

Basically, the algorithm performs the decoding of a codeword, extracting an estimated group of  $N$  bits  $v'$  that is checked by means of syndrome-computation; if the syndrome equals zero, the algorithm considers  $v'$  to be the correct codeword; otherwise it performs another iteration adjusting the values of the a posteriori probabilities by using some internal values computed in the previous iteration. The maximum number of iterations allowed,  $B$ , is a parameter of the algorithm.

This algorithm does not search for the closest codeword compared to the received sequence, but tries to correct every bit. Due to this property, the number of error bits after the decoding is always smaller than the one of error bits prior the decoding, when the algorithm is convergent. Extensive simulation performed by the authors confirmed this property, which might lead to the decrease of error-packet length, that should be corrected by the RS code that follows the LDPC or convolutional codes in many applications.

## II. PERFORMANCES OF LDPC-CODED SINGLE CARRIER TRANSMISSIONS

In order to evaluate the performances of the LDPC codes, we will determine the BER vs. SNR performances of a 2-PSK modulation coded with the proposed code on an AWGN channel.

The BER performances are determined by computer simulation, rather than by theoretical estimation in order to obtain a more realistic evaluation of the LDPC codes behaviour.

The code rates chosen were approximately  $R = 0.75, 0.5, 0.33$  and  $0.2$  in order to allow a comparison with the convolutional codes and turbo codes of rates  $R = 3/4, 1/2, 1/3$  and  $1/5$ .

There are two ways of changing a LDPC code rate:

a) by changing the code parameter  $j$ , for given values of parameters  $k$  and  $p$  (see family F1 below);

b) by shortening the same code, namely decreasing the number of information bits (see family F2 below).

The two families of codes presented in table 1 are based on the "parent" code LDPC ( $k = 14, j = 3, p = 31; N = 434, C = 93, J = 341$ ). This code was selected to fulfill two requirements: to have a good "correction capability" and to have short code words, so they could be employed in multi-user transmissions. Family F1 was obtained by changing the parameter  $j$  of the "parent code" (method a.), while family F2 was obtained by shortening the "parent code" (method b.).

TABLE I  
THE LDPC CODES PARAMETERS EMPLOYED IN SIMULATIONS.

F1	j	N	C	R	F2	j	N	C	R
C <sub>11</sub>	Non-coded			1	C <sub>21</sub>	Non-coded			1
C <sub>12</sub>	3	434	93	0.78	C <sub>22</sub>	3	434	93	0.78
C <sub>13</sub>	7	434	217	0.50	C <sub>23</sub>	3	186	93	0.5
C <sub>14</sub>	9	434	279	0.35	C <sub>24</sub>	3	143	93	0.35
C <sub>15</sub>	11	434	341	0.21	C <sub>25</sub>	3	118	93	0.21

Both families include the non-coded transmissions for reference.

BER vs. SNR performances of the 2-PSK coded with codes of family F1 are displayed in figure 1, and those of 2-PSK coded with codes of family F2 are displayed in figure 2.

The simulations were performed for  $10^6$  information bits for each value of the SNR, and the SNR was modified with a step of 0.5 dB. Due to these facts, the SNR required for BER =  $10^{-6}$  indicated by the simulations, has an error of +/- 0.5 dB. The maximum number of iterations/codeword of the decoder was B= 15.

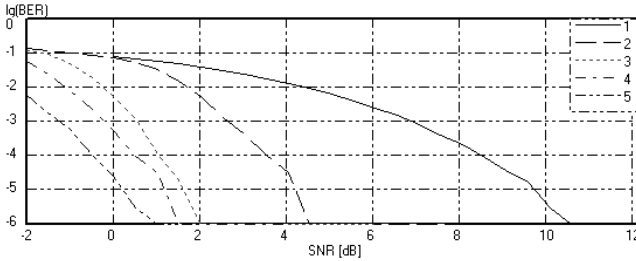


Fig. 1. BER vs. SNR of 2-PSK coded with the LDPC codes of family F1

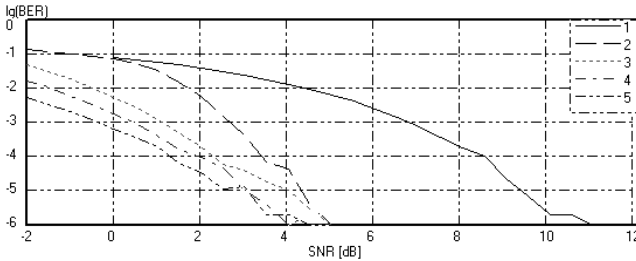


Fig. 2. BER vs. SNR of 2-PSK coded with the LDPC codes of family F2

The coding gains (at BER =  $10^{-6}$ ) provided by the two families are summarized in table 2.

TABLE 2  
CODING GAINS PROVIDED BY THE LDPC CODE FAMILIES OF TABLE I AND FIGURES 1 AND 2.

Code	C <sub>11</sub>	C <sub>12</sub>	C <sub>13</sub>	C <sub>14</sub>	C <sub>15</sub>
C <sub>G</sub> (dB)	-	6	8.5	9	9.5
Code	C <sub>21</sub>	C <sub>22</sub>	C <sub>23</sub>	C <sub>24</sub>	C <sub>25</sub>
C <sub>G</sub> (dB)	-	6.5	6.5	6.5	6.5

Analyzing the coding gains provided by the codes of family F1, we see that the coding gain provided by the “parent code” (R = 0.78) is about 6.5 dB, comparable to the ones provided by the convolutional codes of R = 1/2 and K = 5 – 7, and the R = 1/2 LDPC code provides a coding gain of 8.5 dB, larger than the one the convolutional codes. Considering that the Message Passing decoder has about the same implementation complexity as the 64-state Viterbi decoder, we may conclude

that the LDPC codes provide about the same coding gain as the convolutional code at a higher rate, and a higher coding gain at the same rate.

As compared to the turbo codes, the R = 1/2 LDPC code ensures BER =  $10^{-6}$  at a SNR = 2 dB, about 1 dB higher than the turbo-codes [5], but it requires only one MAP decoder instead of two decoders (MAP + MLD) and a de-interleaver.

Decreasing the code rate by changing the code parameter j, family F1, we get additional coding gains of up to 3.5dB, the most powerful code C15 requiring a SNR= 1dB for BER= $10^{-6}$ .

The simulations performed by the authors showed that a larger coding gain could be obtained by using a code with greater value of p; this would imply longer code words that would complicate the implementation and would not be suitable for multi-user transmissions.

The performances of family F2 codes are poorer at the same rate, due to the fact that the number of control equations in which a bit is involved is always j = 3, compared to j = 7, 9 or 11 for the codes of family F1 (see codes C13 – C23). Due to the fact that j is constant, regardless the rate, the coding gain is practically the same.

The coding gains could be improved by increasing the maximum number of iterations/codeword performed by the Message-Passing decoder; simulations showed that increasing B = 25, leads to an extra coding gain of about 1 dB, at the expense of a longer processing time required.

### III. MULTI-CARRIER CODED TRANSMISSIONS EMPLOYING QAM-SIGNAL CONSTELLATION

#### A. Bit Mapping

When the LDPC-coded bits are to be modulated on a b-bit/symbol QAM constellation, the b-tuple is mapped on the I and Q coordinates of the QAM vector, by splitting the b-tuple into two groups of b/2 bits, each group being assigned to one axis. The bits that are assigned to an axis are mapped to the amplitude levels of that axis according to a Gray encoding [1]. Since the transmission bit-loading might involve non-coded information bits, they are also mapped according to a separate Gray encoding, in order to maximize the distance between levels having the same non-coded bits. Therefore, the multibit assigned to an axis of the QAM constellation, coded and non-coded bits, is mapped according to a double Gray encoding described in [3]. Figure 3 presents an example of mapping b/2 = 4 bits on one axis (I or Q) of a QAM constellation.

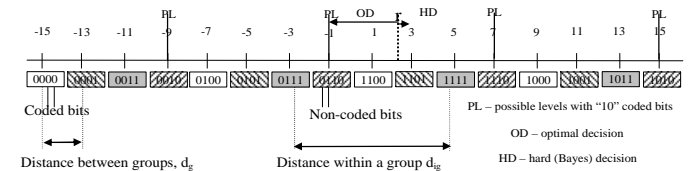


Fig. 3. BER Bit mapping on a constellation axis and optimal decision of the non-coded bits

The amplitude levels employed on each axis belong to the

set A defined by:

$$A = \{A_l = 2l - (L_b - 1), l = 0, 1, \dots, L_b - 1; \}; L_b = 2^{b/2}; \quad (8)$$

This bit-mapping method, which allows only for the employment of the square QAM constellations, is simpler because the mapping is identical on both coordinates.

### B. Soft-Demapping

Because the MP algorithm requires the *a posteriori* probabilities of each bit and the received vector carries more bits, a soft-demapping [3] is required in order to provide the  $F_n^0(0/r)$  and  $F_n^1(1/r)$  probabilities of each bit mapped the received vector.

For multibit/symbol modulations, the two probabilities of each bit are extracted, from the received level on the I or Q branches, by (9) that gives the probability of bit  $b_j$  to be „1” when the demodulated level on a branch equals  $r$  and the channel is AWGN [1]:

$$F_j^1 = \frac{\sum_{l=1}^{2^{b/2}} \exp\left(-\frac{(r-L(l))^2}{2\sigma^2}\right) \cdot b_{lj}}{\sum_{l=1}^{2^{b/2}} \exp\left(-\frac{(r-L(l))^2}{2\sigma^2}\right)}; j = 0, \dots, b/2 - 1; \quad (9)$$

In (9)  $b_{lj}$  denotes the logical value of  $j$ -th bit of the  $l$ -th modulating level of the I or Q branch of the demapped vector. A similar expression is derived for  $F_j^0$  and the two values are normalized to their sum.

The soft-demapping requires a previous estimation of the noise variance  $s$ ; computer simulations run by the authors showed that estimation errors of less than 2 dB, between the actual channel noise variance and the one stored in the soft-demapper, lead to insignificant decreases of the decoder performances.

### C. Soft Decision of the Non-Coded Information Bits

The information non-coded bits mapped on a QAM symbol can be decided by two methods, namely:

- hard decision, applying the Bayes criterion to the probabilities provided by the soft-demapping; this method does not employ the information provided by decoding the coded bits placed on the same tone during the same symbol period.

- soft decision, that considers the information provided by the decoding of the coded bits mapped on the same QAM symbol and tone.

Basically, the optimal decision memorizes the received level  $r$  and, using the decoded bits provided by the LDPC decoder, selects the closest (in the  $d_E$  sense) level that was mapped with the same decoded bits, see figure 3. This method provides lower BER of the non-coded bits, as resulted from simulations performed by the authors, but may error the non-coded bits if the corresponding coded bits were wrongly decoded.

### D. Bit-loading on a Multi-Carrier Transmission

Denoting by  $T$  the number of available tones, by  $T_i$  the

number of tones in group  $i$ , by  $G$  the number of tone-groups, by  $N_{ci}$  and  $N_{ni}$  the numbers of coded and non-coded bits on the  $i$ -th tone and by  $R$  the LDPC code rate, the payload of the transmission would be:

$$D = \sum_{i=1}^G T_i (N_{ci} R + N_{ni}); \quad (10)$$

In order to take advantage of the correction capability of the LDPC code, it is advisable to maintain the largest constellation ( $U$  bits/symbol) employed in the non-coded configuration that ensures the desired bit rate, i.e. observe (11), even at the expense of a slight decrease of the payload. This is because doubling a QAM constellation requires an additional 3 dB of SNR, which diminishes the coding gain provided by the coded configuration.

$$\sum_{i=1}^G T_i (N_{ci} + N_{ni}) \leq T \cdot U; \quad (11)$$

The employment of different numbers of coded and non-coded bits on the same QAM-symbol offers the third possibility of adapting the coded modulation rate. The rate of the coded modulation is computed by:

$$R_{CM} = \frac{N_{ci} \cdot R + N_{ni}}{N_{ci} + N_{ni}}; \quad (12)$$

Considering the 256-QAM ( $N_{ci} + N_{ni} = 8$  bits), some possible configurations using non-coded bits are presented in table 3 together with the rates and coding gains they provide. The LDPC code employed is ( $k = 14, j = 3, p = 31; R = 0.78$ ), which provided a 6.5 dB coding gain on a 2-PSK modulation (code  $C_{12}$  in table 1 and figure 1). The BER vs. SNR performances are presented in figure 4.

TABLE 3  
CONFIGURATIONS USING CODED AND NON-CODED BITS ON A 256-QAM (LDPC – 14,3,31).

No	$N_{ci}$	$N_{ni}$	$R_{CM}$	$C_G$	No	$N_{ci}$	$N_{ni}$	$R_{CM}$	$C_G$
1	0	8	1	-	4	6	2	0.835	6.5
2	2	6	0.945	5	5	8	0	0.780	7
3	4	4	0.890	6					

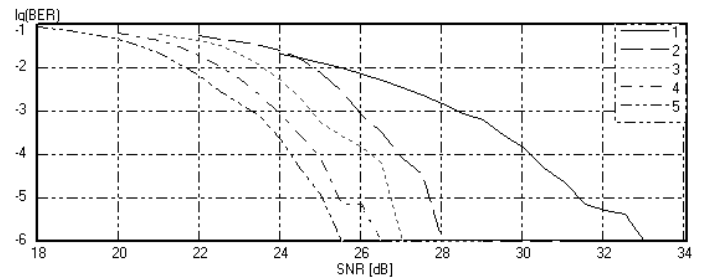


Fig. 4. BER vs. SNR of configurations defined in table 4

The employment of non-coded bits leads to a significantly

increase of the coding rate, e.g. from 0.78 to 0.945, at the expense of a coding gain decrease of about 1-2 dB. This could be explained by the “protection” of the non-coded provided by the 2-level Gray mapping and by their soft decoding.

The effects of these two factors upon the performances of this type of configurations is shown by analyzing separately the BER vs. SNR for both coded and non-coded bits before the MP decoding, for the coded bits, and soft decision, for the non-coded bits, and after these decoders. The BER prior to decoding was obtained by using a hard Bayes decision that employs the *a posteriori* probabilities provided by the soft-demapping. The curves correspond to configuration no.3 from table 3.

Figure 5 shows the BER vs. SNR of the coded and non-coded bits before the MP decoding, for the coded bits, and soft decision, for the non-coded bits, and after these decoders. The BER prior to decoding was obtained by using a hard Bayes decision that employs the *a posteriori* probabilities provided by the soft-demapping. The curves correspond to configuration no.3 from table 3.

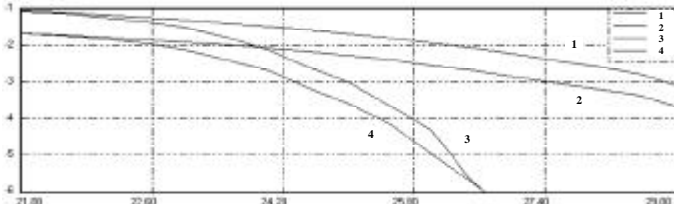


Fig. 5 BER vs. SNR of the coded and non-coded bits of configuration no. 3 from table 3  
(line1 – coded bits Bayes decision; line 2 – non-coded bits Bayes decision;  
line 3 – coded bits MP decoding; line 4 – non-coded bits soft decoding)

As shown in figure 5, the non-coded have lower BER than the coded bits, both before the decoding and after it (line 1 vs. line 2. line 3 vs. line 4). This is due to 2-level Gray mapping of the coded and non-coded bits.

The number of error bits is always smaller after the decoding process, than before it. This, combined with additional investigations performed by the authors indicate that the two decoders might require some smaller outer codes (small RS or even BCH) in FEC schemes employing concatenated codes

#### IV. PERFORMANCES OF THE LDPC-CODED ADAPTIVE MODULATION SCHEMES IN MULTI-CARRIER TRANSMISSIONS

##### A. Simulation Environment and Parameters

The simulation program, developed by the authors, that implements the LDPC-coded multi-carrier transmissions, allows the following parameters to be set: LDPC code parameters ( $k, j, p$ ), number of tone-groups  $G$ , number of tones within a group  $T_i$ , bit-loading for each group ( $N_{ci}, N_{ni}$ ), maximum number  $B$  of iterations/codeword of the LDPC decoder, range and step of SNR, test length.

It displays the BER values and the BER vs. SNR characteristic for the selected SNR range, the number of coded bits error after the decoding of each codeword, and the number of non-coded bits decided by soft-demapping.

The simulations were performed on a test of  $10^6$  information bits and the maximum number of  $B = 15$  iterations/codeword for the decoding algorithm.

##### B. Simulation Performances of LDPC-Coded OFDM Transmissions

###### 1) Non-Coded Transmission Scheme

We shall consider a OFDM transmission that is based on a bin (allocated to one user) of  $T_i$  tones and  $F$  OFDM symbol periods, thus containing  $T_s = T_i \times F$  QAM symbols, out of which only  $A_s$  are “active” symbols being used for the payload. The guard interval (cyclic prefix) is denoted by  $G$  and represents a fraction of the symbol period, the number of bits/QAM symbol is  $n_i$  (it defines the QAM constellation employed), the bin rate is  $D_b$  and the CRC (required for channel estimation-prediction) is  $t$  bits long.

Considering these, the nominal payload for constellation  $i$  ( $n_i$ ), i.e. the maximum value for the payload when SNR is very high, is:

$$D_{ni} = \frac{1}{1+G} \cdot \frac{A_s}{T_s} \cdot D_b \cdot T_s \cdot n_i \cdot \left(1 - \frac{t}{A_s \cdot n_i}\right) \quad (13)$$

Considering the particular values proposed in [6], namely  $D_b = 1500$  bins/sec,  $T_s = 120$  symbols,  $A_s = 108$  symbols,  $G = 0.11$ ,  $t = 8$  bits and  $n_i = 1, 2, 4, 6, 8$  the BER vs. SNR curves of the transmission were obtained by simulation and displayed in figure 6.

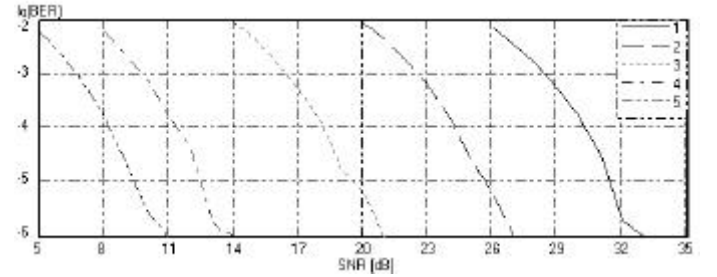


Fig. 6 BER vs. SNR for non-coded 256 (1), 64 (2), 16 (3), 4 (4) QAM and 2-PSK (5)

The constellations having an odd number of bits/symbol (except  $n_i = 1$ ) were not considered for three reasons:

- When it comes to adaptive change of the modulation, the SNR thresholds would be too close (about 3 dB) leading too often to a changing procedure;
- The 8, 32, 128-QAM would require different mapping on the two coordinates that would complicate the implementation.
- The 32 and 128-QAM are cross-constellations that are known to exhibit some synchronization problems

The values of the nominal throughputs of the non-coded schemes, computed using (13) are displayed in table 4.

TABLE 4  
VALUES OF THE NOMINAL PAYLOAD FOR NON-CODED 256, 64, 16, 4-QAM AND 2-PSK

$n_i$	8	6	4	2	1
$D_{ni}$ (kbps)	1156.76	864.86	572.97	281.08	135.13

The throughput (effective payload) is computed considering that only correctly received bins are useful, i.e.:

$$\theta_{ni} = D_{ni}(1 - \text{BinER}_{ni}) \quad (14)$$

In (14),  $\text{BinER}_{n_i}$  denotes the bin error probability of the non-coded configuration using  $n_i$  bits/symbol. The simulation program computes this probability by dividing the number of error bins to the number of received bins.

The curves  $T_{n_i}$  vs. SNR are shown in figure 7, for  $n_i = 8, 6, 4, 2, 1$

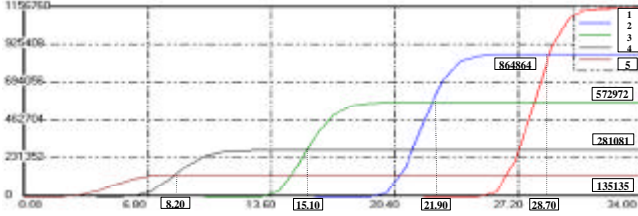


Fig. 7  $T_{n_i}$  vs. SNR for non-coded 256 (1), 64 (2), 16 (3), 4 (4) QAM and 2-PSK (5)

The flat portions of the curves can be explained by the fact that, for SNRs larger than the SNR required for  $\text{BER} < 10^{-6}$  (the test length is 1 million bits), the simulation program counts no bit and bin errors, and so the second factor of (14) equals 1.

The threshold values that separate the regions within which each modulation is optimum are determined by graphical calculations, due to the fact that the SNR variation step was set to 1dB. Their approximate values are depicted on figure 7.

## 2) Coded Transmission Scheme

Since the OFDM transmissions are reported to have poor performances without coding, the  $\text{BER}_{c_i}$  vs. SNR and  $T_{c_i}$  vs. SNR performances of the coded configurations should be evaluated as well.

In order to keep the coding as “sparingly” as possible, the (14, 3, 31) LDPC code with rather high rate ( $R = 0.78$ ) was chosen and, in order to further increase the rate, coded and non-coded bits were mapped on the QAM symbols.

Considering (12), (13) and (2), the ideal payload of the coded configuration  $D_{c_i}$  is expressed by:

$$D_{c_i} = \frac{1}{1+G} \cdot \frac{A_s}{T_s} \cdot D_b \cdot T_s \cdot n_i \cdot \left(1 - \frac{jP}{A_s \cdot n_i}\right); \quad (15)$$

The last factor in (15) is the rate of the coded bin, i.e. the number of information bits over the number of transmitted bits.

The throughput of the coded configurations can be computed by (16),  $\text{BinER}_{c_i}$  denotes the bin error probability of the coded scheme that employs  $n_i$  bits per QAM symbol.

$$\theta_{c_i} = D_{c_i} (1 - \text{BinER}_{c_i}) \quad (16)$$

For flexibility and a simpler implementation, each bin contains a codeword.

The bin-error rate of a configuration employing LDPC-coded bits and non-coded bits is difficult to compute theoretically. Hence, instead of using  $(1 - (1 - p_{\text{post}})^{A_s \cdot n_i})$  ( $p_{\text{post}}$  denoting the post-decoding and decision bit-error probability)

to compute the probability of error bins, we took the values of the bin error probability provided by our simulation program, using a large number of bins as samples.

The transmission configurations employed are listed in list 1, below.

1. non-coded:  $n_1=8; n_{c1}=0; n_{n1}=8; N_c=868; N_n=0; R_{CM}=1$ ; 256-QAM;
2. coded:  $n_1=8; n_{c1}=4; n_{n1}=4; N_c=432; N_n=432; R_{CM}=0.892$ ; 256-QAM
3. coded:  $n_1=6; n_{c1}=4; n_{n1}=2; N_c=432; N_n=216; R_{CM}=0.856$ ; 64-QAM;
3. coded:  $n_1=4; n_{c1}=4; n_{n1}=0; N_c=432; N_n=0; R_{CM}=0.784$ ; 16-QAM;
4. coded:  $n_1=2; n_{c1}=2; n_{n1}=0; N_c=216; N_n=0; R_{CM}=0.57$ ; QPSK

List 1. Coded configurations employed

In the last configuration, the “parent” code was shortened to  $N_c = 216$ , see (4), in order to match the bin capacity. In this way, the same code is employed for all constellations employed.

The 2-PSK modulation was not considered because the bin capacity would be of 108 payload bits, too small to “carry” a powerful codeword. Besides, the coded QPSK configuration provides a 5 dB coding gain compared to non-coded QPSK, see figures 8 and 6, meaning that it provides better performances than non-coded 2-PSK, which has a “coding gain” of 3 dB, compared to non-coded QPSK, as shown in figure 6.

Figure 8 shows the BER vs. SNR curves of the configurations of list 1.

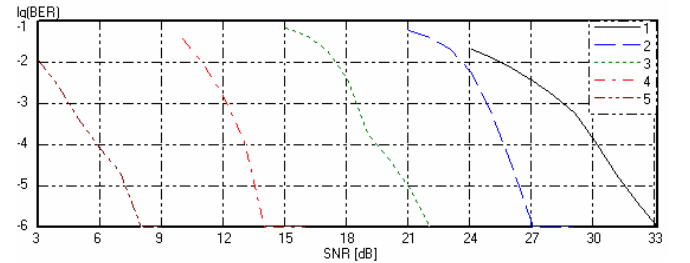


Fig. 8 BER vs. SNR for 256-nc (1), 256-c (2), 64-c (3), 16-c (4) and 4-c QAM (5)

Comparing the SNR required for  $\text{BER} = 10^{-6}$  by the non-coded and coded configurations, we get for the 256-QAM constellation a coding gain of about 6 dB (line 2-fig.8 – line 1 –fig.8 or line 1 fig.6).

For the other QAM constellations the coding gains (line 3-fig.8 – line 2-fig.6 for 64-QAM, line 4-fig.8 – line 3-fig. 6 for 16-QAM and line 5-fig.8 – line 4-fig.6 for 4-QAM) are shown in table 5.

TABLE 5  
CODING GAINS OF CODED QAM CONFIGURATIONS VS. CORRESPONDING NON-CODED QAM CONFIGURATIONS

Constellation	256	64	16	4
$C_G$	6	6	8	6

There should be noted that the simulations were performed using a 1 dB of the SNR. In fact the BER difference between 4 and 16 QAM is about 6.3 dB and this difference decreases at 6

dB as the two constellations compared grow. Due to these two reasons, the 8 dB coding gain of the 64-QAM should be interpreted as a 6-6.5 dB.

The 3 dB coding gain of the coded 4-QAM referenced to non-coded 2-PSK (line 1-fig.3 – line 1-fig.1), which justifies the employment of the coded 4-QAM instead of non-coded 2-PSK, should also be noted.

The coded configurations require no CRC for the channel state estimation-prediction, since the Message-Passing decoding algorithm performs the syndrome check only as a control and this syndrome check can be employed as a CRC.

The nominal payloads  $D_{ci}$  of the five configurations of list 1, computed using (15) for the bin parameters and configurations parameters (list 1) mentioned above, are displayed in table 6.

TABLE 6  
VALUES OF THE NOMINAL PAYLOAD FOR NON-CODED 256 AND CODED 256, 64, 16, AND 4-QAM

$n_i$	8-nc	8-c	6-c	4-c	2-c
$D_{ci}$ (kbps)	1157.76	1041.89	750.0	458.1	166.21

In order to compare the effective payload of the coded configurations, the throughput vs. SNR characteristics of these configurations were computed using (15) and (16) and are displayed in figure 9. The approximate threshold values are depicted on the figure, as well.

In order to compare the effective payload of the coded configurations, the throughput vs. SNR characteristics of these configurations were computed using (15) and (16) and are displayed in figure 9. The approximate threshold values are depicted on the figure, as well.

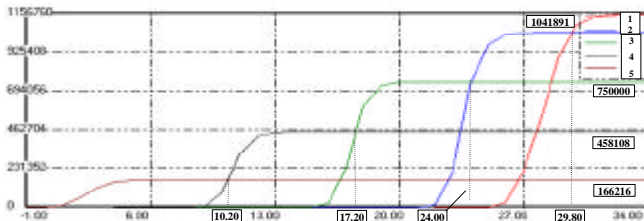


Fig. 9  $T_{ni}$  vs. SNR for 256-nc (1), 256-c (2), 64-c (3), 16-c (4) and 4-c QAM (5)

The distance between the thresholds of the non-coded scheme is about 6.8 dB (see fig.7), and the distance between the thresholds of the coded scheme is 6.8-7dB (see fig.9), except for the highest last threshold, which is 5.8 dB away from its predecessor. This distance ensures that the coded modulation scheme is not changed too often

Considering some SNRs that belong to the same regions defined by the non-coded and coded schemes, figures 7 and 9, we get the values of table 7.

The first column is identical since at high SNRs it's not efficient to employ a code. Results of table 7 show that the coded configurations provide a throughput greater with at least 20% than the corresponding non-coded configurations

TABLE 7  
COMPARISON BETWEEN THE THROUGHPUTS OF THE NON-CODED AND CODED CONFIGURATIONS

SNR (dB)	31.5*	25.5	19.5	13.5	7.5
$T_{nc}$ -kbps	1157*	867	573	281	135
$T_c$ -kbps	1157*	1042	750	458	166
$T_c/T_{nc}$	1	1.20	1.30	1.63	1.23

Also, for low SNRs, the SNR may be decreased about 2 dB (135 kbps at about 4.8 dB), in order to obtain the smallest payload of the non-coded variant, which is provided by the 2-PSK (line 5 in figure 7).

## V. CONCLUSIONS

The array-based LDPC codes employed in the present paper allow for a simple encoding and a moderate complexity decoding, compared to the turbo codes.

The BER performances of the single carrier LDPC-code QAM modulations are close to the ones provided by the similar modulations coded with turbo codes at the same rate and the same number of iterations per code word. A BER =  $10^{-6}$  at SNR = 2 dB in an AWGN channel can be obtained by an R = 0.5 LDPC-coded 2-PSK, ensuring a coding gain of about 9 dB.

When employed on a multi-carrier transmission scheme the LDPC decoder requires the *a priori* knowledge of the channel's noise variance.

A very flexible rate changing LDPC-coded scheme can be obtained by using a bit-loading that combines coded and non-coded bits. The rate can be increased from R = 0.75 up to R = 0.94 at the expense of a 1.5 dB coding gain loss.

Due to the behavior of the LDPC-decoding algorithm and to the soft-decision of the non-coded bits, the authors estimate that small and high rate RS outer codes should be employed in FEC schemes based on concatenated codes.

The LDPC-coded adaptive modulation scheme proposed in the paper ensures coding gains of about 6 dB, compared to the correspondent non-coded scheme.

It also provides an increased throughput, the average increase being of about 20-25%, as compared to the non-coded scheme which employs the same constellations

## REFERENCES (SELECTED)

- [1] – ITU-T, “LDPC codes for G.dmt.bis and G.lite.bis,” Temporary Document CF-060.
- [2] – D.J.C. McKay, “Good error-correcting codes based on very sparse matrices,” IEEE Trans. on Information Theory, vol. 45, No. 2, March, 1999.
- [3] – R. Gallager, “Low-density parity-check codes,” IRE Trans. Information Theory, vol. IT-8, January 1962.
- [4] – ITU-T, “Low-density parity-check codes for DSL transmission,” Temporary Document BI-095.
- [5] – Cl. Berrou, A.Glavieux, “Near Optimum Error Correcting Coding And Decoding: Turbo-Codes”, IEEE Transactions on Communications, vol.44, pp. 1261-1271, October 1996
- [6] – W. Wang, M.Sternad, T. Ottosson, A. Ahlen, A. Svensson, - „Impact of Multiuser Diversity and Channel Variability on Adaptive OFDM“